Numerical calculation of ferrofluid optical transmission evolution after magnetic field switch-on

Ángel SANZ-FELIPE *, Juan Carlos MARTÍN

Applied Physics Dept., University of Zaragoza, C/ Pedro Cerbuna, 12, 50009 Zaragoza (Spain).

*Corresponding author

Abstract

A method to calculate the optical transmission evolution of a ferrofluid after exposure to an external magnetic field is proposed. In the first part of this work, a simulation program is employed to simulate the nanoparticle rearrangement for different particle concentrations and different magnetic field intensities. In the second part, the simulated particle distributions' optical response is determined by means of a mixture law, which avoids typical huge computational times associated to this stage of the calculation. Experimental and simulated results with both parallel and perpendicular magnetic field orientations with respect to the incident light are compared. A significant correlation is obtained, which proves the usefulness of the proposed method in order to obtain the optical transmission evolution of a ferrofluid.

Keywords: Ferrofluid simulation, magneto-optical evolution, mixture law, transmission calculation

1. Introduction

Ferrofluids are colloidal suspensions of magnetic nanoparticles immersed in a carrier fluid. In presence of an external magnetic field, the particles tend to form chains parallel to the field lines [1]. This effect induces changes in the optical properties of these media such as optical absorption variations or even dichroism and rotatory power in some particular cases [1–3]. Control of these properties makes these substances interesting face to potential photonic applications such as variable attenuators or optical magnetic sensors where the ferrofluid entails the basic functional media [4–6].

Once the magnetic field is applied, both the magnetic response and the consequent optical effect depend on many ferrofluid intrinsic parameters (particle's size and magnetization, stabilizing coating, concentration, etc.) as well as on the measurement conditions (magnetic field intensity and relative orientation, light wavelength). This complexity causes a wide diversity of experimental results reported in the literature, which may present even opposite trends under the same magnetic field orientation: an increase [7–9] or a decrease [7,8,10] of the optical transmission after magnetic field application. This variety is even observed with the same sample depending on the magnetostatic field intensity [1,2] or the light wavelength [11]. However, there is a lack of a complete model capable of predicting this diversity of optical behaviors departing from the ferrofluid parameters or measurement conditions, which makes it difficult to

anticipate the final magneto-optical response (if the sample reaches a stable state), and even more difficult to predict its time evolution.

As a consequence, numerical simulations are frequently used to analyze the dynamics of this process. Many authors have simulated the particle rearrangement in chains departing from the mutual interactions between particles under the presence of an external homogeneous magnetic field [12–15]. Most of the works are aimed to verify the particles aggregation and chain coalescence process [16,17]. Others study more specific characteristic such as the influence of particles polydispersity [18,19], the different analytical modeling of the repulsive coating action [15,20], the aging process of the particles which may change their response [18], or other research areas such as thermodynamics [21]. However, not many of them have been extended to deduce the corresponding optical response. Those which study the optical effects are based on calculating the area projected by the particles in the light direction to determine the optical attenuation through scattering models such as the Mie theory [22], or directly calculating the propagation of a plane wave [23]. Due to the limitations of these theories or the difficulty of specifying exactly the characteristics and conditions of the real ferrofluid, determining the correlation between the magnetic effect and the optical consequence is not an easy task, and sometimes only a qualitative study of trends related to the magnetic processes is possible [24]. It is remarkable that the main obstacle for any adequate calculation of light propagation through the sample by means of the typical numerical methods is the computational time which any kind of software would require. It implies that the above mentioned works which delve into the magneto-optical calculation are only applied to any particular step of the ferrofluid evolution, but cannot be extended to calculate the response evolution itself since it would imply unaffordable computational times.

In this work, an alternative method is proposed in order to calculate the optical transmission evolution of a simulated ferrofluid without the need for long calculation times. First, the magnetic response of a ferrofluid as a consequence of the application of an external magnetic field is simulated. Then, a mixture law is employed to estimate the corresponding transmission changes. Its application to optical transmission calculation in ferrofluids has been previously studied [25], with good results. The law requires the determination of an equivalent average aspect ratio of the formed chains, which is one of the key points of this work. Finally, the transmission of the simulated ferrofluid at each evolution step is obtained with such minimal calculation time that it is negligible compared to the magnetic response calculation time. Predicting the magneto-optical response of any ferrofluid by means of this procedure is not the aim of this work since there are too many parameters involved which are difficult to know exactly. Our aim is to verify whether this numerical procedure allows us to obtain the experimentally observed behaviors by finding a theoretical-to-experimental concordance so that the magneto-optical response is adequately reflected by the entire simulation, which could be a useful tool for optimizing the characteristics of ferrofluids face to potential photonic applications.

The paper is organized as follows. Section 2 is devoted to present the particle evolution program employed and the simulations carried out with it. In Section 3 the theoretical mixture law model is explained as well as the procedure to obtain the optical transmission evolution corresponding to the previous simulations. Section 4 presents the comparison between the experimental transmission results obtained with the reference

ferrofluid and those obtained by applying the procedure explained in Section 3 to simulations from Section 2. This comparison will allow us to verify whether the evolution program and the method to calculate the corresponding transmission are adequate.

2. Evolution of nanoparticle distribution: numerical simulation

2.1. Numerical method and considerations

A computer program developed by us [26] has been used to simulate the nanoparticle distribution evolution immediately after magnetic field switch-on. The most relevant interactions between particles are calculated in order to obtain the evolution of their positions, speeds, and magnetic dipole orientations. The program takes into account the dipole-dipole interactions which lead the particles to form chains along the magnetic field lines. The effect of the particle coating is also simulated as a repulsive interaction which prevents them to aggregate in an irreversible way. Resultant forces and torques suffered by the particles are calculated at the beginning of each simulation step. This allows calculating the linear and angular acceleration so that the new position, speed and dipole orientation of every particle are obtained at the end of each step. In order to do so, Brownian and friction effects are considered, as detailed in next subsections. The new data are taken as starting conditions for the next simulation step, and so on. This way, the evolution of particles is simulated.

The simulation cell is a cube of 5.2 μm edge. This size has been selected from the compromise between simulating the highest possible number of particles and taking an assumable computational time. In order to carry out comparisons to experiments, the nominal parameters of the sample employed in [26] have been introduced to the program. Particles have been considered as spheres with a magnetic core of magnetite with radius $R_n = 50$ nm (saturation magnetization $M_s = 30$ emu/g indicated by the manufacturer, density 5170 kg/m^3 [27]). This value has been considered after TEM imaging of the particles [25]. A spherical polymeric coating (density 983.6 kg/m^3, calculated from its composition fully detailed in [25,26]) surrounds the magnetic core so that the complete particle has a hydrodynamic radius $R_h = 92$ nm (as indicated by the manufacturer, measured by DLS technique). The particle polydispersity, PdI = 0.176, indicates that the sample is close to being considered monodispersed, so particles have been simulated as identical spheres for simplicity. The superparamagnetic behavior of the magnetic cores have been checked by measuring the $M - H$ curve [28], so they are monodomain and it is valid to assign the saturation magnetization value to each particle in the simulation. For Brownian and friction effects, viscosity considered in the simulations is $\eta = 1$ mPs, as a reference value corresponding to water at 20ºC.

Nevertheless, the particle coating is not spherical at all but consists of a complex, irregular polymeric structure. As a consequence, parameters which account for friction and Brownian motion are difficult to assess. In addition, all those phenomena entail a delay in the particle evolution and a high number of simulation steps will be required to simulate a long enough particle evolution and chain formation. An important problem in this type of numerical methods is its computational time. In order to overcome all these difficulties and to minimize the computational time, some considerations are taken into account, as detailed below.

2.1.1. Rotational dynamics

In this subsection, we analyze the numerical treatment of two effects: rotational Brownian dispersion and rotational friction.

The rotational Brownian motion is the only interaction in the ferrofluid which opposes the mechanical alignment of the particles' magnetic dipoles, which is the main cause of particle aggregation. Thus, it is decisive for the chain formation process but also a key factor to its dependence on the magnetic field intensity. It has been included in the program as a random angular displacement of the particles orientation in each simulation step, whose mean value is determined by the rotational Brownian diffusion coefficient $D_r = k_B T / 8\,\pi R_h^3\,\eta$ [29]. Figure 1 compares two calculations either neglecting or considering the Brownian effect. They have been carried out with 182 particles within the simulation cell (corresponding to a particle concentration of 7 mg/mL). The time interval used corresponding to a simulation step is $\Delta t = 10$ μs, so the particle movements can be considered infinitesimal. The magnetization M_x of the simulated ferrofluid along the magnetic field direction (X direction) is presented. Its value is shown normalized to the case that all the particles are ideally aligned with the field lines: $M_x = 1$ represents a perfect alignment and $M_x = 0$ represents the state when particles are randomly oriented just before the switch-on.

As shown in Figure 1(a), if rotational Brownian motion is neglected, magnetization becomes saturated no matter the magnetic field intensity, which would also lead to a long-term optical response not dependent on the magnetic field intensity. In contrast, if Brownian motion is considered, Figure 1(b), a clear magnetic dependence of the final M_x appears: the lower the magnetic field, the further the particles' magnetic dipoles are from being perfectly aligned, so the attractive forces and the consequent aggregation are expected to be lower. As experiments show that the magnetic field intensity does have an influence on any stage of the optical response of this sample [25], long-term included, the conclusion is clear: rotational Brownian motion must be considered in numerical simulations. Non-monotonous behavior observed in Figure 1(b) can be attributed to the effect of Brownian movement on an extremely low number of particles, compared to a realistic case: with more than 10^{20} particles, M_x curves would appear as totally smooth and monotonous.

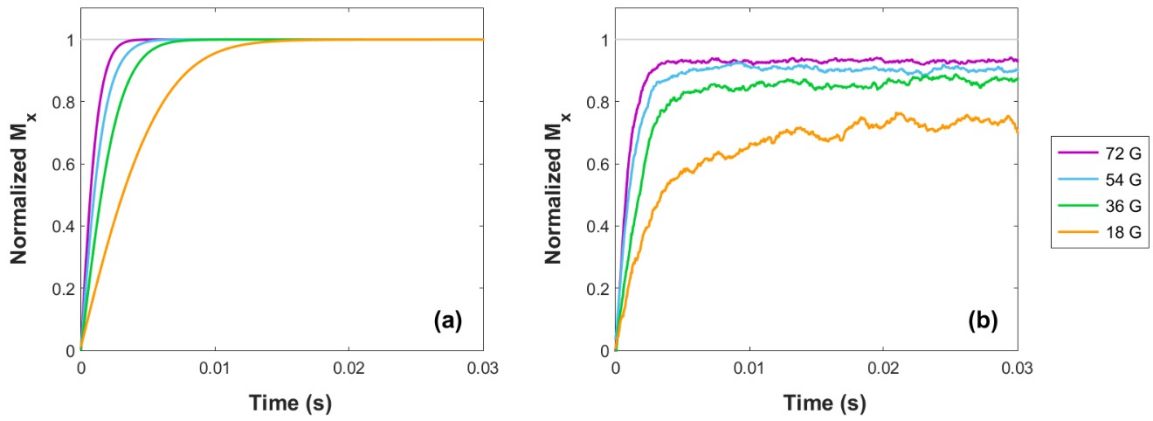

Figure 1.- Evolution of the simulated ferrofluid magnetization along the magnetic field direction (X direction) as a function of the magnetic field intensities when rotational Brownian motion is (a) neglected and (b) considered. Magnetization is normalized with respect to the value in which the particle dipoles were perfectly aligned.

Regarding the rotational friction, profiles and proportions relating the different $M_x(t)$ series depend on the rotational drag coefficient, γ_r, which relates rotational drag torque and angular velocity in the well-known Stokes law: $\vec{\tau}_d = -\gamma_r \vec{\omega}$. As mentioned above, the particles are not spherical but irregular and even with a complex micellar structure. In addition, the viscosity of the carrier fluid (water and SDS surfactant) may be somewhat different to that of water, which have been considered as a reference value in the simulations. Therefore, the average effective γ_r coefficient cannot be easily assessed beforehand. For this reason, in further comparisons between numerical and experimental results, the average rotational drag is considered a fitting parameter. In Figure 1(b) calculations, a value $\gamma_r = 30\gamma_{r,S}$ has been employed, being $\gamma_{r,S} = 8\pi R_h^3 \eta$ the Stokes drag coefficient of a sphere with the particle average hydrodynamic radius [29]. Eventually, this value provides the best fit to the experimental results, as will be seen in Section 4. As it could be expected, its value is much higher than the corresponding to a spherical particle.

2.1.2 Translational dynamics

Concerning translational Brownian motion, it has been incorporated to the simulation program the same way as the rotational contribution: a random displacement can be added at each simulation step, with a mean value determined by the translational Brownian diffusion coefficient $D_t = k_B T / 6\pi R_h \eta$ [29]. In our simulations, inclusion of this effect simply gives rise to a delay: the optical transmission evolution curves obtained with and without translational Brownian motion are the same, save for their different time scales. With regard to the drag coefficient γ_t in the translational Stokes law, $\vec{F}_d = -\gamma_t \vec{v}$, its influence is the same as the translational Brownian motion: we find in our numerical simulations that changes in the γ_t value do not modify the optical transmission curves obtained, save for their different time scales. On the other hand, it deals with a parameter whose previous measurement is very difficult, for the same reasons mentioned above about γ_r. For all these reasons, we treat both translational effects together, by means of an effective γ_t coefficient to be determined by a fitting procedure. This way, explicit simulation of the translational Brownian motion is avoided in the final version of the numerical program, which entails a notable reduction of computational time.

Besides, handling γ_t as a fitting parameter turns out to be very simple as its relationship with time scale is simply proportional. There is a straightforward mathematical justification for that: at each instant along the system evolution, the acceleration of each particle can be calculated as:

$$\vec{a} = \vec{a}_0 - \frac{\gamma_t}{m}\vec{v} \tag{1}$$

where $\vec{a}_0$ accounts for the effect of the different interactions and the last term accounts for the friction effect (being m the particle mass). The displacement $\Delta\vec{x}$ during an infinitesimal interval Δt can be found by integration:

$$\Delta\vec{x} = m\vec{a}_0 \frac{\Delta t}{\gamma_t} + \left(\frac{m^2}{\gamma_t^2}\vec{a}_0 - \frac{m}{\gamma_t}\vec{v}_i\right)\left(e^{-\gamma_t \Delta t/m} - 1\right) \tag{2}$$

being $\vec{v}_i$ the initial speed of the particle. If the quotient $\gamma_t \Delta t/m \gg 1$, the second term on the right can be neglected compared to the first, so this expression becomes:

$$\Delta\vec{x} \cong m\vec{a}_0 \frac{\Delta t}{\gamma_t} \quad (3)$$

The time interval in our simulations is $\Delta t = 10$ μs, so that $\gamma_t \Delta t/m = 3.2\times10^3$ in our sample considering the Stokes drag coefficient for a sphere with the particle average hydrodynamic radius, $\gamma_{t,S} = 6\pi R_h \eta$ [29]. Therefore, this approximation is valid in our simulations and it will also be fulfilled by higher γ_t values. According to this expression, scaling the numerical time and γ_t by the same factor does not affect the amount of the particle displacements and, eventually, does not modify the optical response profile.

A fitting γ_t significantly greater than that of Stokes law is expected: the fitting drag coefficient must account for the Brownian delay effect, the average friction of particles much less hydrodynamic than a sphere and any possible deviation from the reference water viscosity considered in the program. Nevertheless, according to equation (3), using the same Δt step time interval, an identical Δx displacement can be obtained either simulating n steps with $\gamma_t = n\gamma_{t,S}$ or simulating just one step with $\gamma_t = \gamma_{t,S}$. However, the latter case needs a smaller number of steps and so it would allow us to reduce the computational time needed by a factor n. Several tests have been carried out to verify the validity of this relationship in our simulations. Thus, in order to minimize our computational time, the value of the equivalent drag coefficient employed in calculations is that of a sphere with radius R_h. Only in Section 4, in which numerical calculations will be fit to experimental results, the effective γ_t characteristic of the sample studied will be found. Once this value is obtained, the real timescale will be directly obtained by simply multiplying by n the original simulation timescale.

On the other hand, if the actual translational drag were high enough, the chain formation degree could be reduced: the displacements due to the resulting attraction between two particles far enough away could then be comparable to or smaller than the Brownian ones. Nevertheless, several tests have been carried out to verify that this effect does not occur in our simulations, and the only consequence is a delay in the particle evolution. For that reason, the assumptions taken in the previous paragraphs are possible.

2.1.3. Lateral coalescence

The program developed does not account for the possible lateral coalescence of chains [26]. Every particle generates a magnetic field corresponding to its magnetic dipole. When a second particle is near enough as occurs when they get chained, the field lines of both particles are modified. For a long chain with a high number of particles, this effect turns the lateral repulsion of the dipole-dipole forces to be negligible, and then Van der Waals attractive forces lead the chains to coalesce. Taking into account all these considerations in a manageable model is a challenge still to be overcome. Apart from that, it would involve a more complex code and probably a much longer computational time. As a result, our program only accounts for the initial chain formation when all the chains are short enough so that the coalescence is not relevant yet.

2.2. Simulations

Two examples of simulations are shown in Figure 2. They have been carried out with a homogeneous magnetic field of 72 G and two different particle concentrations: 7 and 3.5 mg/mL of particle mass per solution volume, which correspond to 182 and 91 particles in the simulation cell. These two particle concentrations are labeled as (1) and

(2) respectively. The time interval corresponding to a simulation step is $\Delta t = 10$ μs, so the particle rotational and translational displacements can be considered infinitesimal. Since the realistic time scale of our simulations has yet to be adjusted in Section 4, the results in this section will be presented as a function of the simulation steps. Simulations have been stopped after 90000 simulations steps so that a complete evolution of the ferrofluid response takes place, as will be seen later. The evolution after the first 50000 steps has been observed as small enough to consider it as approximately saturated. Since our program does not account for lateral coalescence of chains as mentioned above, no more than 90000 steps are necessary: it would result in a proportional increase in calculation time and, furthermore, the chain coalescence could have already started so that our simulations would not be correct. At step 0, particles are randomly distributed as it occurs in the dispersed ferrofluid in absence of magnetic field, Figure 2(a). Then, the magnetic field is applied along the X direction and the simulation starts running. The particles distributions after 10000 and 50000 simulation steps are shown in Figure 2(b) and 2(c) respectively. As the sample evolves, chains grow and join up to 15 particles in the longest case. The higher the concentration, the lower the average mutual distances between particles and, therefore, the longer the chains, as expected.

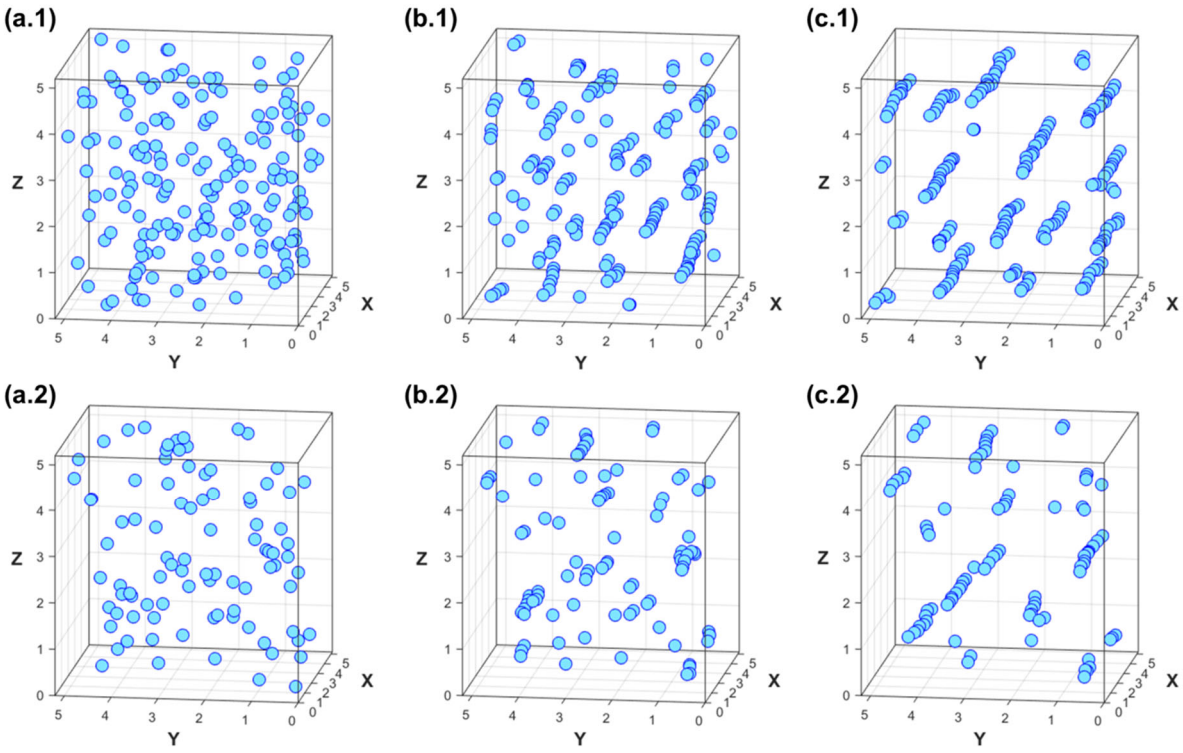

Figure 2.– Simulated ferrofluid cubic cell with the particle distribution at steps 0, 10000 and 50000, (a), (b) and (c) respectively. Two particle concentrations have been simulated, $\varphi = 7$ and 3.5 mg/mL, indicated by labels (1) and (2) respectively. Axes units specified in microns.

Additionally, a set of simulations with four magnetic field intensities with the highest nanoparticle concentration has also been carried out (omitted in this point for simplicity). The corresponding results will be shown later.

2.3. Evolution of the chains' average aspect ratio

In order to analyze the particle evolution and the chain formation, a code is incorporated to the program to obtain information of the chains' aspect ratio evolution, which will be also useful for further transmission calculations. The aspect ratio of any particle chain is defined here as the ratio of its width to its length. The particles' shadow cast on the YZ plane transverse to the magnetic field direction is calculated. Consider the spherical individual particles in the initial dispersed distribution. When N particles become chained along the X direction due to the ferrofluid's magnetic response, the total shadow projected on the YZ plane is reduced by N as they overshadow each other. Since our program does not account for lateral coalescence, chains are formed with one particle in thickness, so that the chain aspect ratio would also be reduced by N in an ideal case. Thus, a parameter K related to the average chain's aspect ratio can be determined as the quotient between the area projected by the particles at any simulation step and that of step 0 when spheres are dispersed. The relationship between K and the aspect ratio in this simplified approach will be better refined in Section 3.

This method could present a problem: the initial randomly distributed particles can somehow overshadow each other so that the initial projected area may not correspond to the transverse particle section multiplied by the total number of particles, but to a value somewhat smaller. It can also happen during the particle evolution between two particles (or chains) that are partially eclipsed by occupying a close YZ position, but totally separated in the X direction and, therefore, far from being chained. However, the simulated cell thickness and the particle concentrations employed are small enough, and this effect has been checked to be negligible in our simulations.

Figure 3 presents the evolution of the area projected by the particles on the YZ plane (colored in black) from Figure 2 simulations. Particles in Figure 3(a) are randomly distributed (step 0), and begin to get overshadowed as they evolve and form longer chains, Figure 3(b) and 3(c), so the total projected area is clearly reduced.

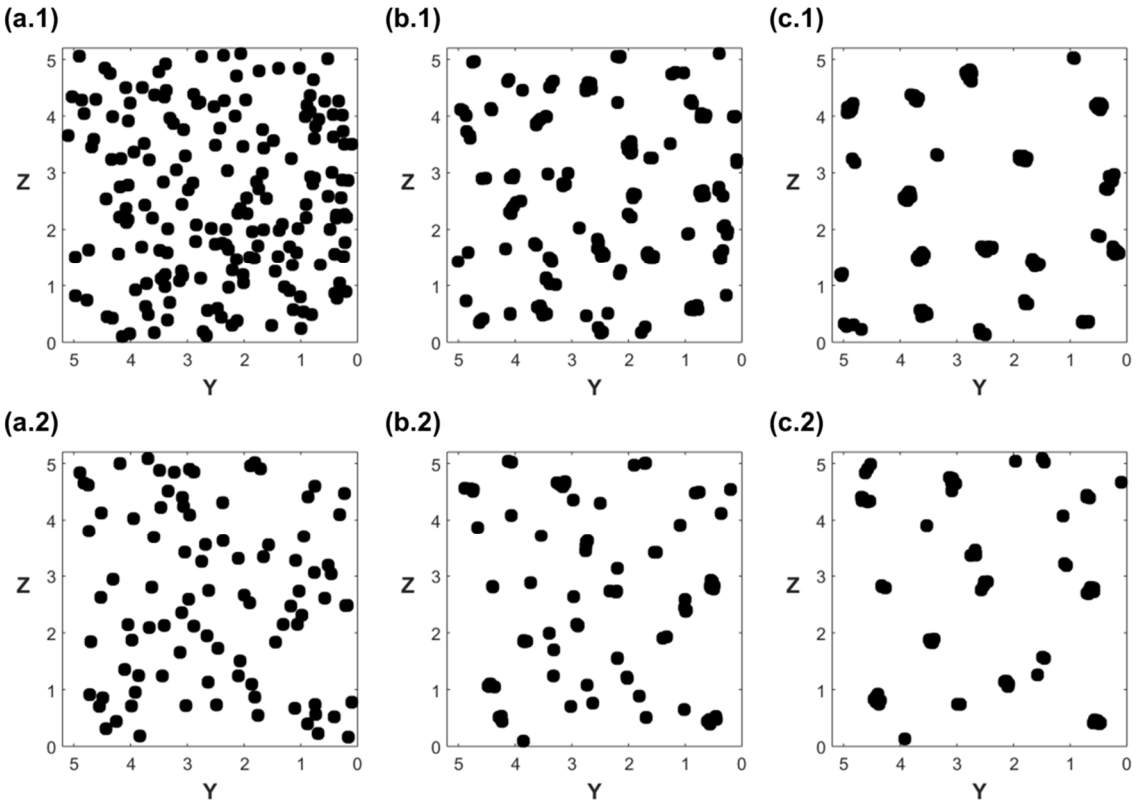

Figure 3.– Area projected by the particles from Figure 2 simulations on the YZ plane transverse to the magnetic field direction. Figures (a), (b) and (c) correspond to simulation steps 0, 10000 and 50000 respectively, with particle concentrations $\varphi = 7$ and 3.5 mg/mL, indicated by labels (1) and (2) respectively. Axes units specified in microns.

Figure 4 shows the K parameter evolution of Figure 3 results. It clearly decreases after magnetic field switch on, as expected due to the chain formation. As the sample evolves, the change slows down: the chain formation begins to be stabilized since particles are already chained and it is more difficult to attract new particles that are further away. Regarding the dependence on nanoparticle concentration, the higher the concentration, the longer the chains formed (as observed in Figure 2), and therefore the greater the change in the K parameter.

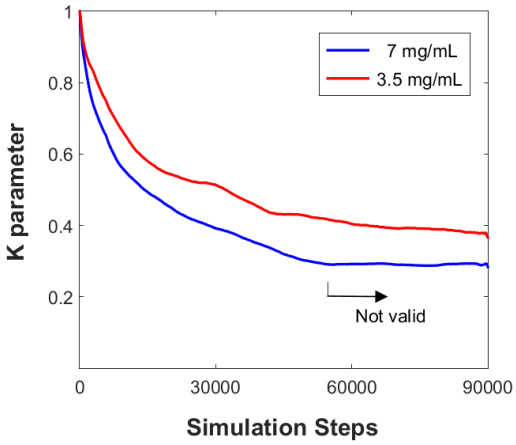

Figure 4.– Evolution of the K parameter in simulations of Figure 3.

As indicated in Figure 4, after approximately 54000 simulation steps, the particle evolution cannot be taken into consideration: the longest chains formed have reached the limits of the simulation cell so that the system evolution stops being realistic. This is clearly observed in the highest concentration but also in some chains for the lowest one. For that reason, only results up to 54000 simulation steps will be considered from now on. In order to avoid this limitation, it would be required to increase the simulation volume, what would increase proportionally the total number of nanoparticles. The computational time in our program is approximately proportional to the square of the number of particles, so that it would take an unaffordable computational time. As an example to contextualize it: Figure 4 simulations took around a total of 55 hours in a conventional computer. Obviously, this time depends on the available computer and the code optimization; we just provide it in order to give a limit about the magnitude of the calculations. Anyway, the chains formed after this number of steps are of considerable length (see Figure 2(c)), and coalescence may already be significant. Since our program does not account for coalescence, the evolution might not be realistic even if the simulation volume and steps were increased. Thus, the volume employed has been considered convenient, and it will be checked when analyzing the results if it adequately reflects the initial magneto-optical response of the ferrofluid before lateral coalescence may occur.

In addition, simulations with magnetic field intensities of 54, 36 and 18 G have been carried out with the highest particle concentration. The aim of these simulations is to check the ferrofluid evolution dependence on the magnetic field intensity under identical conditions, and the capability of the numerical method and the considerations mentioned in subsection 2.1 to simulate the ferrofluid experimental response. The K parameter evolution results are presented in Figure 5. It is observed that the higher the field intensity, the more reduced the K parameter, that is to say the longer the chains are formed in average. This is consistent with Figure 1(b) results: the higher the magnetic field, the more aligned the particles' magnetic dipoles and, as a consequence, the more intense the mutual attractive interactions that lead to chain formation.

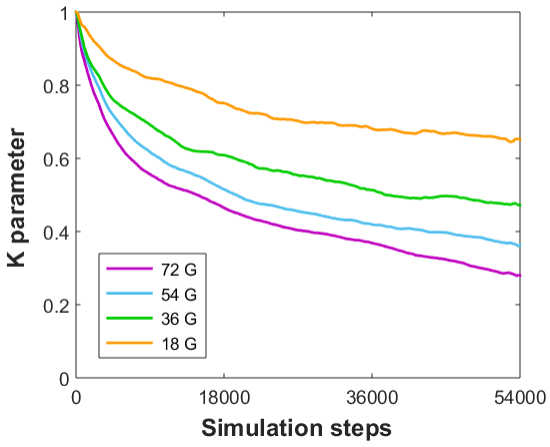

Figure 5.– Evolution of the K parameter in simulations using different magnetic field intensities (particle concentration $\varphi = 7$ mg/mL).

3. Optical transmission calculation

Looking at Figure 3, it could be assumed that light transmission would be greater when the particle chains are formed as there is a larger space through which the light would not find any obstacle. However, as it will be seen in experimental results in Section 4, this assumption is not correct in our sample (and similar results in the literature). The particle size and even the chain size are lower or comparable to the wavelength of interest ($\lambda = 632.8$ nm), or those for possible photonic applications (visible and near infrared). Therefore, light scattering in these systems is highly dependent on sizes, wavelength, chain formation and materials' refractive indices [30]. Simple ray tracing approaches found in the literature are not adequate: although they can be adapted to reflect the results, they are usually based on theories that are not completely valid for these systems [31]. On the contrary, the calculations proposed in this work attempt to simulate phenomena that do occur in the ferrofluid.

Calculating the optical transmission of these particle distributions could be faced by means of theoretical models which consider the parallel [32–34] or perpendicular [32,35] orientation of chains with respect to the incident light. These models are typically quite complex and would require a high precision in the ferrofluid parameters to obtain adequate quantitative results. On the other hand, numerical software for calculating the propagation of an electromagnetic pulse, typically by means of finite integration methods, usually requires long computational times for just one particle distribution at a specific time step [24]. Therefore, determining the transmission evolution of the ferrofluid would take an unaffordable time. As a solution, we propose the use of a mixture law to deduce the transmission changes and evolution departing from the K parameter obtained in Section 2. Usefulness of this law to relate ferrofluid optical transmission to average chain aspect ratio has already been checked by us in a former paper [25]. This method entails a direct calculation so that no high computational time is required to determine the transmission evolution, and therefore, it could even be implemented within the particle evolution program from Section 2.

3.1. Mixture law

Mixture laws often refer to formulae which predict the effective optical properties of a mixture of several homogeneous media departing from their characteristics and proportion. Thus, they are useful for estimating the optical properties of ferrofluids: inclusions (particles or aggregates of them) immersed in a continuous phase (carrier fluid). An adaptation of the Maxwell-Garnett formula [36] is considered in order to account for inclusions with ellipsoidal shape and uniform orientation [37]. The effective dielectric permittivity of the mixture in the U direction can be deduced as the host permittivity, ε_e, plus a small contribution due to the inclusions immersed in it:

$$\varepsilon^*_{ef,U} = \varepsilon_e(1 + \chi^*_U) \tag{4}$$

where the term χ_U is given by:

$$\chi^*_U = \frac{p}{N_U(1-p) + b^*} \tag{5}$$

In this expression, $b^* = \varepsilon_e/(\varepsilon^*_i - \varepsilon_e)$, where ε^*_i is the inclusions permittivity, p is the volume fraction occupied by them, and N_U is the ellipsoid depolarization factor in the U

direction [25,37]. Every complex magnitude is denoted by an asterisk, except ε_e in which the imaginary component for water is negligible at the wavelength employed ($\varepsilon_e^* = 1.7739 - 4.41\times10^{-8}j$ [38]). When no magnetic field is applied, particles can be considered statistically spherical so that $N = 1/3$ in any calculus direction. When the magnetic field is switched on, the particles gather into chains or somehow ellipsoids of revolution with the polar axis aligned along the field lines. The depolarization factors along the polar and equatorial directions, denoted by $\parallel$ and $\perp$ subscripts respectively, can be calculated departing from the ellipsoid axes [37]. Then, the characteristic depolarization factors of the average ellipsoid which represents the whole variety of shapes in the ferrofluid can be expressed as a function of its aspect ratio $A = r_\perp/r_\parallel$ as follows:

$$N_\parallel = \left[-\pi + 2\sqrt{A^2-1} + 2\,tan^{-1}\left(\frac{1}{\sqrt{A^2-1}}\right)\right]\frac{A^2}{2(A^2-1)^{3/2}}$$
$$N_\perp = \left[\frac{\pi}{2} - \frac{\sqrt{A^2-1}}{A^2} - tan^{-1}\left(\frac{1}{\sqrt{A^2-1}}\right)\right]\frac{A^2}{2(A^2-1)^{3/2}} \quad (6)$$

which satisfy the relationship $N_\parallel + 2N_\perp = 1$. The effective permittivity of the mixture determines its optical attenuation, $\alpha = 2k\mathrm{Im}\left(\sqrt{\varepsilon_{ef}^*}\right)$, so that the optical transmission of a sample of length L can be calculated using the well-known expression $T = e^{\alpha L}$. The volume fraction of nanoparticles in a ferrofluid for optical applications is usually much smaller than one, so that taking into account the typical permittivities of the materials employed, the particles contribution χ^* to the effective permittivity is small. Under this consideration, the ferrofluid transmission when the magnetic field is applied parallel or perpendicular with regard to the light beam ($U = \parallel$ or $\perp$ respectively) can be calculated with the mixture law as [25]:

$$ln\,T_U = \frac{4\pi L}{\lambda}\,Im\left(1 + \frac{1}{2}\frac{p}{N_U(1-p) + b^*}\right) \quad (7)$$

This expression relates the absolute ferrofluid transmission with the particle concentration, the permittivity of both fluid and particles, and the depolarization factor of the average aggregate, which can be obtained from its shape by introducing the aspect ratio in equations (6). In order to apply this theory to the particle arrangements described in Section 2, it is necessary to establish a link between the K parameter obtained there and the aspect ratio representing the ferrofluid state.

3.2. Equivalent ellipsoid aspect ratio

The K parameter obtained in subsection 2.3 provides information about the average aspect ratio of the particle chains within the ferrofluid. Nevertheless, the original mixture law was developed for ellipsoidal inclusions instead of chains of spherical inclusions so the aspect ratio of an equivalent ellipsoid is needed. In addition, in the original law it was considered that all inclusions had the same size, while in the case studied here there are chains of different lengths together with individual particles, whose global contribution requires averaging their effect in a certain way.

On the other hand, it must be taking into account that it exists some separation between consecutive particles due to the coating's repulsive force, and the chains present

an irregular shape caused by the Brownian motion (as appreciated in Figure 2). So, both K parameter and the aspect ratio would be slightly different from an ideal definition. Our proposal in this work is to consider that the differences are small enough so that a linear relationship between K and A can be assumed, and therefore their temporal variations would be proportional:

$$A(t) - A(0) = \delta \cdot \big(K(t) - K(0)\big) \tag{8}$$

Remind that, in absence of chains ($t = 0$), $K(0) = 1$ and $A(0) = 1$. As a result, this expression can be rewritten as:

$$A(t) = \delta \cdot K(t) + (1 - \delta) \tag{9}$$

where δ is a proportionality parameter to be determined by fitting to experimental results. This way, the aspect ratio of an ellipsoid equivalent to the average particle chain is obtained. Anyway, it deals with a purely heuristic assumption whose usefulness can only be validated by comparison between simulations and experiments.

4. Comparison between experimental and simulated results

Experimental results have been obtained by means of the setup and procedure detailed in [25], which corresponds to a standard setup for magneto-optical measurements. The sample employed contains magnetite particles (NanoMyp, MagP®) with the specifications already detailed in subsection 2.1. The ferrofluid is contained in a cuvette with dimension 9.5 mm × 36.8 mm × 2 mm (inner light path). Optical transmission evolution of the sample after magnetic field switch on has been registered with both particle concentrations simulated in Section 2, $\varphi = 7$ and 3.5 mg/mL, employing a magnetic field intensity of 72 G and both parallel and perpendicular orientations with respect to the incident light beam ($\lambda = 632.8$ nm). Besides, three more magnetic field intensities (54, 36 and 18 G) have also been applied to the sample with the highest concentration. This way, the conditions of both series of simulations carried out in Section 2 have been experimentally measured.

Permittivities used in mixture law calculations are 1.7739 for the water of the carrier fluid [38] and 3.2388-0.1224j for the particles (obtained as a compromise between the refractive indices and proportions of the materials that compound the magnetic core and stabilizing coating of the entire particle). Three fitting parameters have been employed: γ_r, γ_t and δ. All curves of the series are fit with the same drag coefficients, while the δ parameter is allowed to take a particular value for each curve. For the reasons explained in subsection 2.1.2, the value of γ_t does not alter the curve profiles, but only the time scale, which is finally determined by means of this fit.

Figure 7 shows the results obtained for both particles concentrations under a magnetic field intensity of 72 G in both parallel and perpendicular relative directions. Simulations from Figure 4 have been used to adjust the entire evolution response to the experimental one. The fitting effective drag coefficients are: $\gamma_r = 30\gamma_{r,S}$ (as advanced in subsection 2.1.1) and $\gamma_t = 22\gamma_{t,S}$. These values, remarkably greater than the characteristic of a sphere, $\gamma_{r,S}$ and $\gamma_{t,S}$, are consistent with what could be expected: they account for a drag effect corresponding to particles much less hydrodynamic than spheres

and, besides, the translational coefficient also accounts for the additional delay effect caused by translational Brownian motion. A precise quantitative comparison to any expected value is not possible since there is no theoretical calculation to be matched which considers all these phenomena together. Nevertheless, their validity is supported by the good correlation between experimental and simulating results below. The fitting δ parameters obtained are: $\delta_{\parallel} = 0.51$ and $\delta_{\perp} = 0.67$ for $\varphi = 7$ mg/mL, and $\delta_{\parallel} = 0.48$ and $\delta_{\perp} = 0.66$ for $\varphi = 3.5$ mg/mL ($\delta_{\parallel}$ and $\delta_{\perp}$ correspond to parallel and perpendicular relative orientations of the magnetic field with respect to the light beam). These results present a similar value for both concentrations, and significantly different depending on the relative orientation. As inclusions are not ellipsoidal, the depolarization factor on both parallel or perpendicular orientations, $N_{\parallel}$ or $N_{\perp}$, may present an imperfect match between the experimental transmission results and relationship $N_{\parallel} + 2N_{\perp} = 1$. As a consequence, it is not surprising that some differences arise between the aspect ratio obtained from experimental results in both magnetic field directions [25].

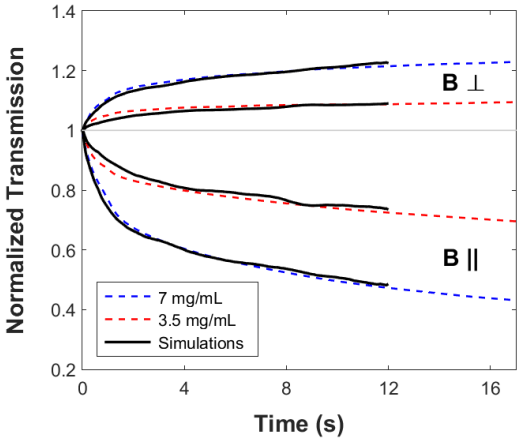

Figure 6.– Comparison between the experimental (dashed line) and simulated (solid line) results of the ferrofluid's optical transmission evolution with both parallel and perpendicular magnetic field orientation with respect to the incident light beam ($B = 72$ G) and with both particle concentrations employed.

It is noteworthy that the four curves in Figure 6, all fit significantly well to the experimental evolution. Besides, once γ_t has been determined, the time scale indicates that the simulation corresponds to the first seconds of the sample response. The effects associated to chain coalescence have been experimentally observed in this sample after several tens of seconds (sample#1 in [24]), when a trend inversion on the transmission evolution is detected. Therefore, Figure 6 results are consistent with the fact that the program only accounts for the initial formation of individual chains of particles. Both remarkable aspects verify, first, the adequate development and fine tuning of the program to simulate the test sample, and second, the feasibility of our proposal to calculate the magneto-optical transmission evolution from the simulations.

On the other hand, Figure 7(a) shows the results obtained with different magnetic field intensities under both relative orientations ($\varphi = 7$ mg/mL). Simulations from Figure 5 have been used to adjust the entire evolution response to the experimental one. As said before, the fitting values of the drag coefficients are the same as for Figure 6. The parameters $\delta_{\parallel}$ and $\delta_{\perp}$ obtained are shown in Figure 7(b). The dependence on the magnetic field intensity reflects significantly well the experimental responses in all cases. The δ

parameters show again a significant deviation between the parallel and perpendicular orientation, which also depends on the magnetic field intensity: the higher the magnetic field, the greater this deviation from the average value. This is consistent with the point already mentioned in Figure 5 discussion: the more intense the magnetic field, the longer the chains are formed and, as a consequence, the more the deviation from an ideal ellipsoidal shape [25]. These results confirm the adequate development of the simulation program as well as the capability of the proposed method to calculate the magneto-optical transmission evolution departing from the simulations.

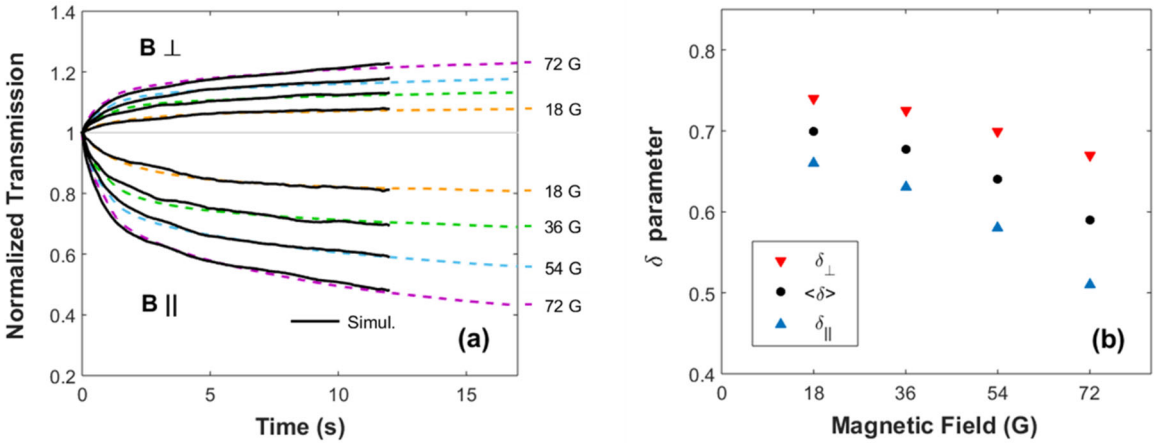

Figure 7.– (a) Comparison between the experimental (dashed line) and simulated (solid line) results of the ferrofluid's optical transmission evolution using different magnetic field intensities under both parallel and perpendicular relative orientations ($\varphi = 7$ mg/mL). (b) Proportionality factor δ as a function of the magnetic field intensity for both relative orientations.

5. Conclusions

A numerical method has been applied to simulate the optical transmission evolution of a ferrofluid after exposure to a magnetic field. Simulations of the particle evolution of a test ferrofluid have been carried out. A procedure based on treating the chain distributions by means of equivalent ellipsoids whose aspect ratio can be easily tracked has been employed to calculate the corresponding optical transmission evolution through a mixture law. Brownian and friction effects have been adapted or offset by comparison to experimental results in order to minimize the computational time. The optical transmission evolution of the simulated ferrofluid fits adequately to the experimental results with the test sample, both for different particle concentrations and for different magnetic field intensities and relative orientations.

On the one hand, the results verify the adequate performance of the particle evolution program employed to simulate the initial formation of particle chains. On the other hand, the good agreement between experimental and simulated results shows up the viability of the method proposed and the approximations considered. Once the sample has been characterized, this procedure allows us to calculate the optical transmission of the ferrofluid at all times with a negligible calculation time compared to that of the magnetic response program, so that it could even be calculated simultaneously to the latter. This way, simulating the initial evolution of the magneto-optical response of a ferrofluid caused by an external magnetic field is feasible in reasonable computational

times. Obviously, a first adjustment is necessary to obtain the fitting parameters, and some parameters or considerations could be further refined in future works. However, these results represent a very interesting starting point to simulate the magneto-optical response evolution avoiding unaffordable computational times and with significantly good results.

Acknowledgements

This work has been supported by the Diputación General de Aragón, project E44_17R.

REFERENCES

[1] Ivey M., Liu J., Zhu Y., and Cutillas S., "*Magnetic-field-induced structural transitions in a ferrofluid emulsion*", Phys. Rev. E **63** (2000) 011403. https://doi.org/10.1103/PhysRevE.63.011403.

[2] Brojabasi S., Muthukumaran T., Laskar J.M., and Philip J., "*The effect of suspended Fe_3O_4 nanoparticle size on magneto-optical properties of ferrofluids*", Opt. Commun. **336** (2015) 278–285. https://doi.org/10.1016/j.optcom.2014.09.065.

[3] Vales-Pinzón C., Alvarado-Gil J.J., Medina-Esquivel R., and Martínez-Torres P., "*Polarized light transmission in ferrofluids loaded with carbon nanotubes in the presence of a uniform magnetic field*", J. Magn. Magn. Mater. **369** (2014) 114–121. https://doi.org/10.1016/j.jmmm.2014.06.025.

[4] Luo L., Pu S., Dong S., and Tang J., "*Fiber-optic magnetic field sensor using magnetic fluid as the cladding*", Sensors Actuators A Phys. **236** (2015) 67–72. https://doi.org/10.1016/j.sna.2015.10.034.

[5] Miao Y., Wu J., Lin W., Zhang K., Yuan Y., Song B., Zhang H., Liu B., and Yao J., "*Magnetic field tunability of optical microfiber taper integrated with ferrofluid*", Opt. Express **21** (2013) 29914. https://doi.org/10.1364/OE.21.029914.

[6] Rodriguez-Schwendtner E., Navarrete M.-C., Diaz-Herrera N., Gonzalez-Cano A., and Esteban O., "*Advanced Plasmonic Fiber-Optic Sensor for High Sensitivity Measurement of Magnetic Field*", IEEE Sens. J. **19** (2019) 7355–7364. https://doi.org/10.1109/JSEN.2019.2916157.

[7] Sanz-Felipe A. and Martín J.C., "Ferrofluids with high dynamic ranges of optical transmission," in *Proceedings of SPIE - The International Society for Optical Engineering* (2017), Vol. 10453, p. 10453P. https://doi.org/10.1117/12.2271794.

[8] Chen L., Li J., Qiu X., Lin Y., Liu X., Miao H., and Fu J., "*Magneto-optical effect in a system of colloidal particle having anisotropic dielectric property*", Opt. Commun. **316** (2014) 146–151. https://doi.org/10.1016/j.optcom.2013.11.058.

[9] Horng H.E., Hong C.-Y., Yang S.., and Yang H.C., "*Novel properties and applications in magnetic fluids*", J. Phys. Chem. Solids **62** (2001) 1749–1764. https://doi.org/10.1016/S0022-3697(01)00108-1.

[10] Laskar J.M., Philip J., and Raj B., "*Experimental investigation of magnetic-field-induced aggregation kinetics in nonaqueous ferrofluids*", Phys. Rev. E **82** (2010) 021402. https://doi.org/10.1103/PhysRevE.82.021402.

[11] Wu K.T., Yao Y.D., and Huang H.K., "*Comparison of dynamic and optical properties of Fe3O4 ferrofluid emulsion in water and oleic acid under magnetic field*", J. Magn. Magn. Mater. **209** (2000) 246–248. https://doi.org/10.1016/S0304-8853(99)00704-0.

[12] Kruse T., Spanoudaki A., and Pelster R., "*Monte Carlo simulations of polydisperse*

ferrofluids: Cluster formation and field-dependent microstructure", Phys. Rev. B **68** (2003) 054208. https://doi.org/10.1103/PhysRevB.68.054208.

[13] Tanygin B.M., Shulyma S.I., Kovalenko V.F., and Petrychuk M. V., "*Ferrofluid nucleus phase transitions in an external uniform magnetic field*", Chinese Phys. B **24** (2015) 104702. https://doi.org/10.1088/1674-1056/24/10/104702.

[14] Tanygin B.M., Kovalenko V.F., Petrychuk M.V., and Dzyan S.A., "*Molecular dynamics study of the primary ferrofluid aggregate formation*", J. Magn. Magn. Mater. **324** (2012) 4006–4010. https://doi.org/10.1016/j.jmmm.2012.07.004.

[15] Wang Z., Holm C., and Müller H.W., "*Molecular dynamics study on the equilibrium magnetization properties and structure of ferrofluids*", Phys. Rev. E **66** (2002) 021405. https://doi.org/10.1103/PhysRevE.66.021405.

[16] Satoh A., Chantrell R.W., and Coverdale G.N., "*Brownian Dynamics Simulations of Ferromagnetic Colloidal Dispersions in a Simple Shear Flow*", J. Colloid Interface Sci. **209** (1999) 44–59. https://doi.org/10.1006/jcis.1998.5826.

[17] Shulyma S.I., Tanygin B.M., Kovalenko V.F., and Petrychuk M.V., "*Magneto-optical extinction trend inversion in ferrofluids*", J. Magn. Magn. Mater. **416** (2016) 141–149. https://doi.org/10.1016/j.jmmm.2016.04.071.

[18] Bakuzis A.F., Branquinho L.C., Castro L.L., Eloi M.T.A., and Miotto R., "*Chain formation and aging process in biocompatible polydisperse ferrofluids: Experimental investigation and Monte Carlo simulations*", Adv. Colloid Interface Sci. **191**–**192** (2013) 1–21. https://doi.org/10.1016/j.cis.2012.12.003.

[19] Solovyova A.Y., Elfimova E.A., Ivanov A.O., and Camp P.J., "*Modified mean-field theory of the magnetic properties of concentrated, high-susceptibility, polydisperse ferrofluids*", Phys. Rev. E **96** (2017) 052609. https://doi.org/10.1103/PhysRevE.96.052609.

[20] Jund P., Kim S.G., Tománek D., and Hetherington J., "*Stability and Fragmentation of Complex Structures in Ferrofluids*", Phys. Rev. Lett. **74** (1995) 3049–3052. https://doi.org/10.1103/PhysRevLett.74.3049.

[21] Jafari A., Tynjälä T., Mousavi S.M., and Sarkomaa P., "*Simulation of heat transfer in a ferrofluid using computational fluid dynamics technique*", Int. J. Heat Fluid Flow **29** (2008) 1197–1202. https://doi.org/10.1016/j.ijheatfluidflow.2008.01.007.

[22] Zhao Y., Lv R.-Q., Li H., and Wang Q., "*Simulation and Experimental Measurement of Magnetic Fluid Transmission Characteristics Subjected to the Magnetic Field*", IEEE Trans. Magn. **50** (2014) 1–7. https://doi.org/10.1109/TMAG.2013.2288228.

[23] Tasker A., Chantrell R.W., Miles J.J., Parker M.R., and Bradbury A., "*Monte-Carlo simulations of light transmission in dispersions of paramagnetic particles*", IEEE Trans. Magn. **24** (1988) 1671–1673. https://doi.org/10.1109/20.11566.

[24] Sanz-Felipe Á., Barba I., and Martín J.C., "*Optical transmission of ferrofluids exposed to a magnetic field: Analysis by electromagnetic wave propagation numerical methods*", J. Mol. Liq. **315** (2020) 113713. https://doi.org/10.1016/j.molliq.2020.113713.

[25] Sanz-Felipe Á. and Martín J.C., "*Analysis of the optical transmission of a ferrofluid by an electromagnetic mixture law*", J. Phys. D. Appl. Phys. **51** (2018) 135001. https://doi.org/10.1088/1361-6463/aab05f.

[26] Sanz-Felipe Á. and Martín J.C., "*Numerical method for analysis of the correlation between ferrofluid optical transmission and its intrinsic properties*", J. Magn. Magn. Mater. **474** (2019) 613–618. https://doi.org/10.1016/j.jmmm.2018.12.026.

[27] Lide D.R., "*CRC Handbook of Chemistry and Physics, Internet Version 2005*" (2005).

[28] Sanz-Felipe Á. and Martín J.C., "*Analysis of temperature dependence in ferrofluid optical transmission dynamics after magnetic field commutation*", J. Magn. Magn. Mater. 529 (2021) 167836. https://doi.org/10.1016/j.jmmm.2021.167836.

[29] Fowler R.H., "*Statistical Mechanics: The Theory of the Properties of Matter in Equilibrium*", 2nd ed. (Cambridge: Cambridge University Press, 1936).

[30] Van de Hulst H.C., "*Light Scattering by Small Particles*" (New York: Dover Publications, Inc., 1981).

[31] Sanz-Felipe Á. and Martín J.C., "*Application of a paramagnetic gas theory to describe the magneto-optical response in ferrofluids*", J. Phys. D. Appl. Phys. **53** (2020) 495106. https://doi.org/10.1088/1361-6463/abb489.

[32] Lee S.-C. and Grzesik J.A., "*Light scattering by closely spaced parallel cylinders embedded in a semi-infinite dielectric medium*", J. Opt. Soc. Am. A **15** (1998) 163. https://doi.org/10.1364/JOSAA.15.000163.

[33] Lou W. and Charalampopoulos T.T., "*On the electromagnetic scattering and absorption of agglomerated small spherical particles*", J. Phys. D. Appl. Phys. **27** (1994) 2258–2270. https://doi.org/10.1088/0022-3727/27/11/004.

[34] Jones A.R., "*Scattering efficiency factors for agglomerates for small spheres*", J. Phys. D. Appl. Phys. **12** (1979) 1661–1672. https://doi.org/10.1088/0022-3727/12/10/007.

[35] Felbacq D., Tayeb G., and Maystre D., "*Scattering by a random set of parallel cylinders*", J. Opt. Soc. Am. A **11** (1994) 2526. https://doi.org/10.1364/JOSAA.11.002526.

[36] Garnett J.C.M., "*Colours in Metal Glasses and in Metallic Films*", Philos. Trans. R. Soc. A Math. Phys. Eng. Sci. **203** (1904) 385–420. https://doi.org/10.1098/rsta.1904.0024.

[37] Sihvola A.H. and Kong J.A., "*Effective permittivity of dielectric mixtures*", IEEE Trans. Geosci. Remote Sens. **26** (1988) 420–429. https://doi.org/10.1109/36.3045.

[38] Kedenburg S., Vieweg M., Gissibl T., and Giessen H., "*Linear refractive index and absorption measurements of nonlinear optical liquids in the visible and near-infrared spectral region*", Opt. Mater. Express **2** (2012) 1588. https://doi.org/10.1364/OME.2.001588.